Ultrahigh-resolution optical coherence tomography with a fiber laser source at 1 μm

Hyungsik Lim, Yi Jiang, Yimin Wang, Yu-Chih Huang, and Zhongping Chen

Beckman Laser Institute and Department of Biomedical Engineering, University of California, Irvine, Irvine, California 92612

Frank W. Wise

Department of Applied Physics, Cornell University, Ithaca, New York 14853

Received December 10, 2004

We report a compact, high-power, fiber-based source for ultrahigh-resolution optical coherence tomography (OCT) near 1 μm. The practical source is based on a short-pulse, ytterbium-doped fiber laser and on generation of a continuum spectrum in a photonic crystal fiber. The broadband emission has an average power of 140 mW and offers an axial resolution of 2.1 μm in air ($<$1.6 μm in biological tissue). The generation of a broad bandwidth is robust and efficient. We demonstrate ultrahigh-resolution, time-domain OCT imaging of *in vitro* and *in vivo* biological tissues. © 2005 Optical Society of America

OCIS codes: 140.3510, 320.7090.

Optical coherence tomography (OCT) permits noninvasive, cross-sectional imaging of biological tissue.[1] The distinct capabilities of the imaging modality are facilitated by the properties of a low-coherence beam. There have been continual efforts in the development of optical sources, as high-power, high-brightness, and broad-bandwidth light sources are essential in high-speed, high-resolution OCT imaging. For artifact-free images, a Gaussian-like spectrum of the beam is desired. Also, practicality of the source is important if OCT imaging is to find use in clinical environments.

Superluminescent diodes are currently popular low-coherence beam sources in clinical OCT systems owing to their compactness and economy. However, semiconductor-based sources typically have a limited spectral width of less than 100 nm, which corresponds to an axial resolution of 10–20 μm. In the past few years, highly nonlinear photonic crystal fibers (PCFs) have drawn attention because femtosecond pulses can generate supercontinuum with bandwidths of several hundred nanometers.[2] Ultrahigh-resolution OCT with a mode-locked Ti:sapphire laser and a PCF has been reported.[3,4]

The depth range of biophotonic imaging, e.g., OCT, is ultimately limited by the penetration of light into biological tissues. The wavelengths for maximum depth range are 1.0–1.3 μm, where the attenuation that is due to absorption and scattering is minimum. A previous study described the use of a mode-locked Nd:glass laser at 1.06-μm wavelength and a high numerical aperture single-mode fiber for ultrahigh-resolution, real-time OCT imaging.[5] The range near 1 μm is particularly interesting in ophthalmology because it offers OCT imaging with minimum dispersion.[6] Currently ophthalmic OCT imaging is done predominantly at ~0.82-μm center wavelength.[7] However, eye-safe exposure at 1 μm is a factor of 3.3 larger than that at 0.82 μm,[8] which permits the use of a higher incident power for ocular imaging. Therefore, with deeper penetration and improved sensitivity, OCT imaging near 1-μm wavelength could be more beneficial than near 0.82 μm.

Bulk solid-state lasers are expensive, and they are cumbersome in clinical OCT applications for which small volume and stable operation of an imaging station are critical. Rare-earth-doped fiber-based systems, which offer lower cost and freedom from the need for alignment, could be practical alternatives. A system based on an erbium fiber and a highly nonlinear fiber has been introduced.[9] However, the wavelength of the mode-locked pulses used in the scheme is far from the targeted center of broadband output. Only a small fraction of the supercontinuum is useful for imaging, and as a result low average power (~4 mW) illuminates the Michelson interferometer. Recently a Raman continuum light source near 1.3 μm with a high-power (10-W) cw ytterbium-doped fiber laser was reported. The novel broadband generation was rather inefficient (3.3%), and it provided 330 mW of power, with 6.3-μm free-space axial resolution for high-speed, *in vivo*, time-domain OCT imaging.[10]

We demonstrate here a fiber-based, compact, high-power source for ultrahigh-resolution OCT imaging in the spectral range near 1 μm. The device exploits high-energy pulses from a practical mode-locked ytterbium-doped fiber laser. Generated with a PCF, the broad spectrum at 1.04-μm center wavelength permits a free-space longitudinal resolution of 2.1 μm. Spectral filtering of the continuum is not necessary, because the wavelength of the short-pulse source is already within the transparency band of tissue. The continuum generation is efficient and delivers a high average power of 140 mW to the interferometer. The utility of the source in an ultrahigh-resolution, time-domain OCT system is confirmed by imaging of biological tissues. The low-coherence beam from the compact fiber device is robust and

0146-9592/05/101171-3/$15.00

stable and therefore is well suited for clinical OCT applications.

The experimental configuration is depicted in Fig. 1. A self-starting, stretched-pulse Yb fiber laser[11] generates ultrashort pulses at a repetition rate of 50 MHz. The net (path-averaged) intracavity dispersion of the oscillator is approximately -0.02 ps^2. The beam from the fiber oscillator is guided into an ytterbium-doped fiber amplifier[12] via a 10% fiber coupler, so the short-pulse part of the system is integrated. Mode-locked pulses are temporally stretched in a 10-m single-mode fiber and amplified in ytterbium-doped fibers pumped with two 980-nm diode lasers, each capable of as much as 500-mW average power (total 1-W average power). After dechirping in external grating pairs (1200 lines/mm), linearly polarized, nearly transform-limited pulses are obtained. The amplified-pulse source in the experiment occupies 30 cm $\times$ 45 cm $\times$ 12 cm, but it can be condensed into a much smaller space. The whole system can be transported conveniently. The PCF (2-m length, 0.2 NA, 5-μm core diameter; from Crystal Fibre A/S) in the experiment has a zero-dispersion wavelength at 1065 nm. The launched pulse is in a small normal-dispersion region of the fiber, so modulational instability is suppressed.[13] A coupling efficiency of 35% is routinely obtained. A half-wave plate controls the input polarization.

We verified the utility of the generated light in ultrahigh-resolution, time-domain OCT by imaging of biological tissues. First we measured the coherence length with a mirror in the probe arm of the interferometer. The reference arm was scanned with a voice coil translation stage with a frequency of 10 Hz. For imaging tissues, a neutral-density filter was inserted to attenuate the reference beam for enhanced sensitivity, and a fused-silica prism pair compensated for the second-order dispersion (Fig. 1).

From the fiber oscillator, mode-locked pulses with a bandwidth of 30-nm FWHM are generated. After the ytterbium-doped amplifier and the grating dechirper, nearly transform-limited pulses were obtained. The dechirped pulse duration was 170 fs, and the average power was 400 mW. The spectral narrowing during the amplification is caused primarily by the finite bandwidth of ytterbium gain [Fig. 2(a), dashed and dotted curves]. Through propagation in the PCF the spectrum was uniformly broadened until it extended from 850 to 1250 nm (Fig. 2, solid curve). The output spectrum is modulated with the center at 1.04 μm. The shallow dip at $\sim$1.06 μm is associated with splitting of soliton and dispersive waves at the zero-dispersion wavelength of PCF.[14] The average power of the continuum was 140 mW, which is 35 times higher than that from the erbium-based fiber source.[9] The continuum generation is stable, and the efficiency ($\sim$35%) was ten times higher than through a Raman process (as was employed in the cw ytterbium-fiber system[10]). We measured the electric-field autocorrelation, and the axial point-spread function yielded 2.1-μm resolution ($<$1.6 μm in biological tissue) with small secondary structures [Fig. 3(a)]. The Fourier transformation from the measured power spectrum is illustrated in Fig. 3(b). The deviation between the temporal and the spectral measurements arises from the spectral responsitivity of the InGaAs photodiode used in the detection.

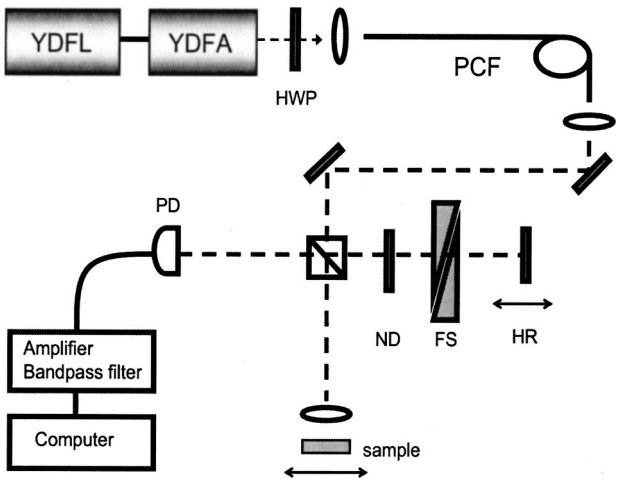

Fig. 1. Experimental configuration: YDFL, ytterbium-doped fiber laser; YDFA, ytterbium-doped fiber amplifier; HWP, half-wave plate; ND, neutral-density filter; FS, fused-silica prisms; HR, high-reflector mirror; PD, InGaAs photodiode.

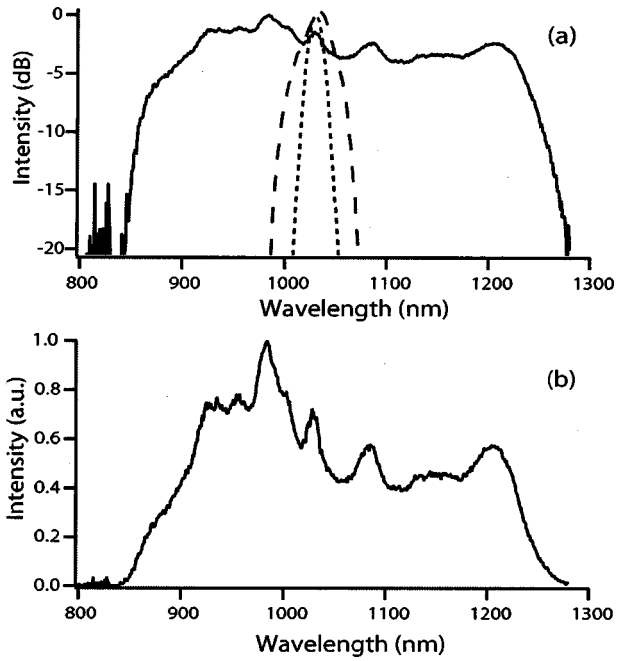

Fig. 2. Spectra of (a) the continuum from a PCF (solid curve), the output from the oscillator (dashed curve), and the amplified pulse (dotted curve) on logarithmic scales; (b) the continuum on a linear scale.

Figure 4 shows three tomograms, which correspond to *in vitro* bovine bone, onion skin, and *in vivo* African frog tadpole, from top to bottom. Figures 4(a) and 4(b) consist of 2000 $\times$ 400 pixels showing areas of 2.0 mm $\times$ 0.4 mm in the samples. In the *in vitro* experiment the mid-shaft portions of bovine femurs were sectioned into 2 cm $\times$ 3 cm blocks and used for imaging. The corresponding OCT image in

Fig. 4(a) shows the surface profile and the highly scattering lamella structures of the bone. In Fig. 4(b), pleomorphic mesenchymal cells in the onion can be identified. In the *in vivo* imaging experiment a 35-day-old tadpole was anesthetized and kept in a water chamber to prevent dehydration. Figure 4(c) consists of 1000×400 pixels showing an area of $1.0\ \text{mm} \times 0.4\ \text{mm}$ near the eye of the tadpole. The highly scattering structures in the cell, such as cell membranes and cell nuclei, as well as nearby tissue morphology, can be seen.

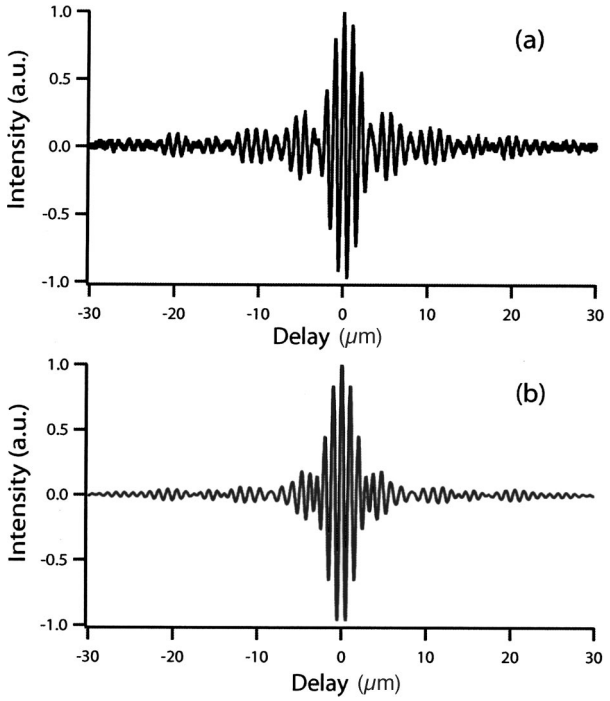

Fig. 3. Autocorrelation: (a) direct temporal measurement and (b) Fourier transform from the measured power spectrum.

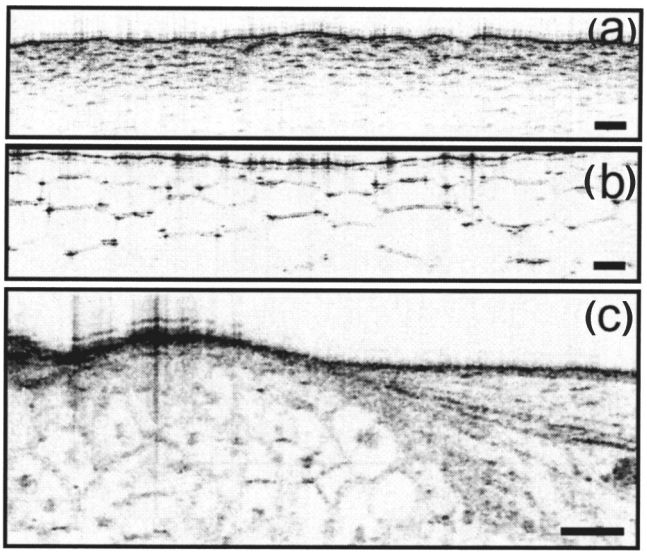

Fig. 4. Ultrahigh-resolution OCT images of biological samples acquired with the system described here: (a) *in vitro* bovine bone, (b) onion skin, (c) *in vivo* African frog tadpole. Scale bar, 100 μm.

In conclusion, we have demonstrated a compact, high-power, fiber-based OCT source in the range near 1-μm wavelength. The device produces a broad bandwidth efficiently and stably, with 35 times higher average power than a previous erbium-doped fiber-based source. The axial resolution is 2.1 μm in air ($<$1.6 μm in tissue). We have demonstrated use of this optical source in ultrahigh-resolution, time-domain OCT imaging of biological tissue. We anticipate that the scheme presented will be implemented with a fiber interferometer in the near future and that the portable system will be valuable in biomedical applications in clinical settings.

The authors gratefully acknowledge support from Tetsuya Endo and D. M. Gardiner of the Department of Developmental and Cell Biology, University of California, Irvine, for preparing the tadpoles. This research was supported by research grants awarded by the National Science Foundation (BES-86924), the National Institutes of Health (EB-00293, EB-002019, NCI-91717, and RR-01192), and the Air Force Office of Scientific Research (FA 9550–04–1–0101). Z. Chen's e-mail address is zchen2@uci.edu.

References

1. D. Huang, E. A. Swanson, C. P. Lin, J. S. Schuman, W. G. Stinson, W. Chang, M. R. Hee, T. Flotte, K. Gregory, C. A. Puliafito, and J. G. Fujimoto, Science **254**, 1178 (1991).
2. J. K. Ranka, R. S. Windeler, and A. J. Stentz, Opt. Lett. **25**, 25 (2000).
3. I. Hartl, X. D. Li, C. Chudoba, R. K. Ghanta, T. H. Ko, J. G. Fujimoto, J. K. Ranka, and R. S. Windeler, Opt. Lett. **26**, 608 (2001).
4. Y. Wang, Y. Zhao, J. S. Nelson, Z. Chen, and R. S. Windeler, Opt. Lett. **28**, 182 (2003).
5. S. Bourquin, A. D. Aguirre, I. Hartl, P. Hsiung, T. H. Ko, J. G. Fujimoto, T. A. Birks, W. J. Wadsworth, U. Bunting, and D. Kopf, Opt. Express **11**, 3290 (2003), http://www.opticsexpress.org.
6. Y. Wang, J. S. Nelson, Z. Chen, B. J. Reiser, R. S. Chuck, and R. S. Windeler, Opt. Express **11**, 1411 (2003), http://www.opticsexpress.org.
7. W. Drexler, J. Biomed. Opt. **9**, 47 (2004).
8. American National Standards Institute, *Safe Use of Lasers*, ANSI Standard Z 136.1 (American National Standards Institute, New York, 1993).
9. K. Bizheva, B. Povazay, B. Hermann, H. Sattmann, W. Drexler, M. Mei, R. Holzwarth, T. Hoelzenbein, V. Wacheck, and H. Pehamberger, Opt. Lett. **28**, 707 (2003).
10. P. Hsiung, Y. Chen, T. H. Ko, J. G. Fujimoto, C. J. S. de Matos, S. V. Popov, J. R. Taylor, and V. P. Gapontsev, Opt. Express **12**, 5287 (2004), http://www.opticsexpress.org.
11. H. Lim, F. Ö. Ilday, and F. W. Wise, Opt. Lett. **28**, 660 (2003).
12. F. Ö. Ilday, H. Lim, J. Buckley, and F. W. Wise, Opt. Lett. **28**, 1362 (2003).
13. J. M. Dudley and S. Coen, Opt. Lett. **27**, 1180 (2002).
14. V. P. Yanovsky and F. W. Wise, Opt. Lett. **19**, 1547 (1994).